Oxygen diffusivities in mullite/zirconia composites measured by $^{18}O/^{16}O$ isotope exchange and secondary ion mass spectrometry

Hong-Da Ko and Chien-Cheng Lin[a)]
Department of Materials Science and Engineering, National Chiao Tung University, Hsinchu 30050, Taiwan

(Received 4 July 2007; accepted 16 August 2007)

Oxygen diffusivities in mullite/zirconia composites were measured by $^{18}O/^{16}O$ isotope exchange and secondary ion mass spectrometry. They exhibited a wide range of values from 10^{-21} to 10^{-10} m^2/s at temperatures between 1000 and 1350 °C in the composites with 0 to 80 vol% zirconia. At a fixed temperature, oxygen diffusivities in high-zirconia composites were larger by at least eight orders of magnitude than those in low-zirconia composites. The percolation threshold occurred between 30 and 40 vol% zirconia, where oxygen diffusivities dramatically changed. There was a clear tendency of the activation energies of oxygen diffusion in composites to decrease with increasing zirconia contents. The large oxygen diffusivities in the high-zirconia composites were attributed to the interconnected channels of zirconia from the microstructural aspect.

I. INTRODUCTION

Mullite-matrix composites are good candidates for high-temperature structural applications among ceramic-matrix composites, because of their low thermal expansion coefficient, excellent strength, and creep resistance at high temperatures, and good thermal shock resistance. Previous studies have reported that partially stabilized zirconia (PSZ) and silicon carbide (SiC) effectively improved the mechanical properties of mullite-matrix composites.[1–4] However, the oxidation of the SiC constituent would deteriorate the mechanical properties of such composites under high-temperature oxidizing environments. Moreover, the oxidation resistance of SiC-reinforced ceramic-matrix composites could be seriously degraded because of the incorporation of PSZ into the matrix.

Several investigations on the oxidation behavior of mullite/PSZ/SiC composites have been carried out.[5–10] In a pioneering study, Lin et al.[10] first phenomenologically proposed two distinct oxidation modes, designated as mode I and mode II, of mullite/PSZ/SiC composites at elevated temperatures: mode I was based on the assumption that oxygen diffusion in the silica layer was much faster than in the mullite/zirconia matrix, and mode II operated otherwise. However, oxygen diffusivities in various mullite/PSZ composites have not been available to date.

All the measurements of oxygen diffusivities in previous studies were conducted on monolithic ceramics.[11–13] Using secondary ion mass spectrometry, Fielitz et al.[11] measured oxygen diffusivities in 2/1-mullite and reported that oxygen diffusivities ranged from 5×10^{-20} to 9×10^{-18} m^2/s at temperatures ranging from 1250 to 1525 °C. Ikuma et al.[12] determined oxygen diffusivities in single crystal mullite to be between 1×10^{-21} and 8×10^{-20} m^2/s at 1100 to 1300 °C. Kim et al.[13] measured oxygen diffusivities in 2.8 mol% Y_2O_3–ZrO_2 to be 3.5×10^{-11} m^2/s at 1000 °C using Raman spectroscopy combined with the ^{18}O–^{16}O isotope exchange technique. In this study, oxygen diffusivities in mullite/zirconia composites with various zirconia contents were measured by the $^{18}O/^{16}O$ isotope exchange method using secondary ion mass spectroscopy (SIMS) to supplement the existing data base of oxygen diffusivities in ceramic materials. The relationship among oxygen diffusivity, composition, and microstructure for various mullite/zirconia composites is elucidated.

II. EXPERIMENTAL PROCEDURE

The starting materials were commercial mullite powder (0.2 μm in average, KM-mullite, Kyoritsu Ceramic Material Co., Nagoya, Japan) and 3 mol% Y_2O_3 partially stabilized zirconia powder (0.3 μm in average, TZ-3Y, Toyo Soda Mfg., Co., Tokyo, Japan). The mullite powder was mixed with various amounts of zirconia. The

[a)]Address all correspondence to this author.
e-mail: chienlin@cc.nctu.edu.tw
DOI: 10.1557/JMR.2008.0073

compositions and designations of the composites are listed in Table I.

The powder mixtures were hot pressed at 1600 °C, except at 1675 °C for the monolithic mullite, in an argon atmosphere and a uniaxial pressure of 30 MPa for 45 min using a hot press (model HP50-HTG-7010, Thermal Technology, Inc., Santa Rosa, CA). Oxygen-deficient zirconia was formed in the as-hot-pressed samples. To avoid the inaccuracy, the samples were preannealed in air at 1360 °C/ 4 h after ultrasonic cleaning in acetone so that stoichiometric zirconia was obtained.

Hot-pressed samples were cut into pieces with dimensions of approximately 10 mm × 6 mm × 3 mm. All of the pieces were ground with a 15-μm diamond matted disc and then polished with 3-μm diamond paste using a precision polishing machine (model Minimet 1000, Buehler Ltd., Lake Bluff, IL). Then microstructures were observed by a field emission scanning electron microscope (FE-SEM, Model JSM-6500F, JEOL, Tokyo, Japan) with an acceleration voltage of 15 kV. To avoid charging, the samples were coated with gold using an ion coater.

The isotope-exchange method was applied using the rare stable isotope ^{18}O (99 at.%, Isotec Inc., Miamisburg, OH) as tracer. Prior to annealing, the samples were rinsed ultrasonically in an acetone bath and distilled water. Then the chamber was evacuated, and a mixture of argon and ^{18}O with the ratio of 4:1 was introduced. The isotope exchange annealing was carried out at 1000 °C/5 h, 1200 °C/3 h, and 1350 °C/2 h, respectively.

The isotope concentration profiles were analyzed using secondary ion mass spectrometry (SIMS, model Quad 6600, PHI, Chanhassen, MN) with Cs ion (5 keV, 100 nA) as the primary beam. The rastered area was 300 μm × 300 μm, and the diameter of the analyzed zone was 75 μm. For the composites with a low-zirconia content (i.e., less than 30 vol% ZrO_2 in this study), the diffusion depth of ^{18}O isotope was quite small, and the ^{18}O concentrations at various depths were measured by sputtering with the Cs ion beam. In the case of the composites with a high zirconia content (i.e., larger than 40 vol% ZrO_2 in this study), the oxygen isotope penetrated deeply into the sample. The sample was then sectioned at various depths, where the ^{18}O concentrations were measured by the method mentioned previously.

III. RESULTS AND DISCUSSION

A. Measured oxygen concentration profiles

The concentrations of oxygen isotope were calculated from the measured secondary ion intensities $I(^{18}O)$ and $I(^{16}O)$ according to

$$C(x,t) = \frac{I(^{18}O)}{I(^{16}O) + I(^{18}O)} \quad . \tag{1}$$

In general, it is better to determine diffusivities under conditions where the steady state is reached. To achieve such experimental conditions (large $\alpha(t/D)^{1/2}$), the measured ^{18}O concentration profiles can be fit by a simple erfc-type equation, while the reliability of the data can be improved by eliminating the surface exchange coefficient α as a fitting parameter. However, shorter diffusion anneal times (small $\alpha(t/D)^{1/2}$) were used in this study to expedite the experiments. Then oxygen diffusivities as well as surface exchange coefficients can be determined under such conditions, when the measured ^{18}O concentration profiles are fitted by the following diffusion solution $C(x,t)$ for a semi-infinite medium given by Crank.[14]

$$\frac{C(x,t) - C_{bg}}{C_g - C_{bg}} = \mathrm{erfc}\left(\frac{x}{\sqrt{4D_v t}}\right) - \exp(hx + h^2 D_v t)\mathrm{erfc} \times \left(\frac{x}{\sqrt{4D_v t}} + h\sqrt{D_v t}\right) \quad , \tag{2}$$

where D_v is the volume diffusion coefficient (m^2/s), α the surface exchange coefficient (m/s), h being equal to α/D_v, C_g the ^{18}O concentration in the gas phase, C_{bg} the natural background level of ^{18}O in the sample (~0.2%), and t the duration of the isotope anneal.

The ^{18}O concentration profiles $C(x,t)$ for various composites annealed at 1000 °C are plotted in Fig. 1. The concentration profiles for MZY40 and MZY80 had a much smaller slope than those for pure mullite and for composites with 30 vol% ZrO_2 or less. The slope of the

TABLE I. Designations, compositions, hot-pressing conditions, and relative densities of various mullite/zirconia composites.

Sample	Composition	HP condition[a]	Relative density (%)
M	Mullite	1675 °C/45 min	97.8
MZY05	95 vol% mullite + 5 vol% 3Y-PSZ	1600 °C/45 min	97.1
MZY15	85 vol% mullite + 15 vol% 3Y-PSZ	1600 °C/45 min	95.1
MZY20	80 vol% mullite + 20 vol% 3Y-PSZ	1600 °C/45 min	95.4
MZY30	70 vol% mullite + 30 vol% 3Y-PSZ	1600 °C/45 min	96.7
MZY40	60 vol% mullite + 40 vol% 3Y-PSZ	1600 °C/45 min	97.5
MZY80	20 vol% mullite + 80 vol% 3Y-PSZ	1600 °C/45 min	97.7

[a]All under the pressure of 30 MPa and 1 atm argon.

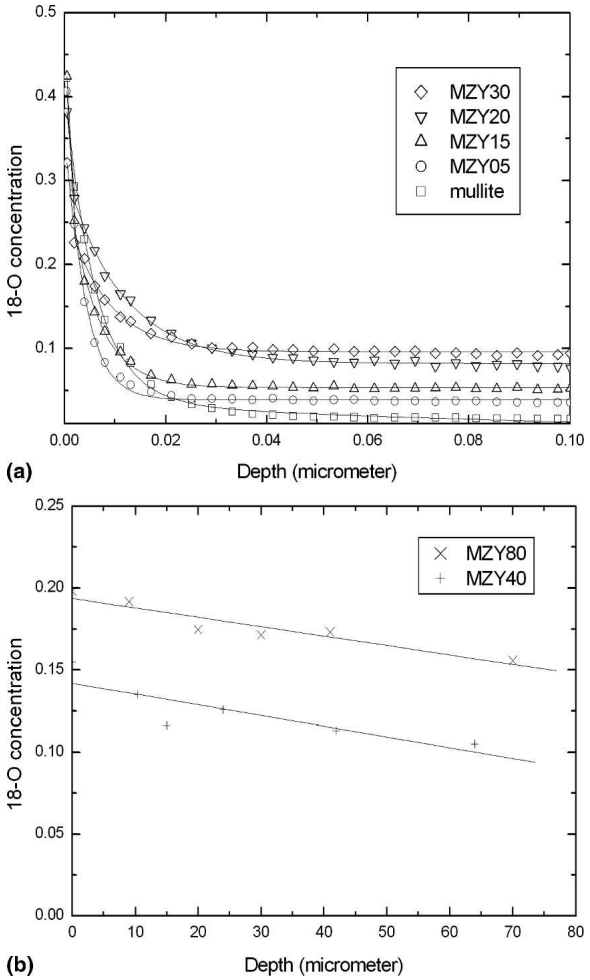

FIG. 1. The concentration profiles of oxygen isotope ^{18}O after annealing at 1000 °C/5 h for (a) mullite, MZY05, MZY15, MZY20, and MZY30; and (b) MZY40 and MZY80.

concentration profile decreased with increasing zirconia content. As shown in Fig. 1(a), the tail for each composite approached a fixed value, which increased with ZrO_2 content. This was probably caused by the fact that the grain-boundary diffusivity in ZrO_2 was much higher than that in mullite. Note that the tail of experimental data in mullite was about 25 times higher than the natural ^{18}O content (0.2%) and about an order of magnitude higher than the grain-boundary-related tail of the diffusion profile as reported by Fielitz et al.[15] This could be attributed to the fact that the grain size (about 0.5 μm) in the current study was considerably smaller than that (about 5 μm) in the previous study conducted by Fielitz et al.[15] The penetration depth of ^{18}O sharply increased as the ZrO_2 content increased beyond some threshold value. Figure 1(b) shows the concentration profiles for MZY40 and MZY80, indicating a penetration depth of more than 70 μm. The ^{18}O concentrations of MZY80 were obviously higher than those of MZY40 at the corresponding depths.

B. Oxygen diffusivities versus zirconia contents

Oxygen diffusivities as well as surface exchange coefficients were determined from the ^{18}O concentration profiles $C(x,t)$, based upon Eq. (2) and nonlinear regression analyses. The results are listed in Table II. The composites were divided into two categories depending on their diffusivities and surface exchange coefficients: the composites with 30 vol% have smaller values for these parameters, and those with 40 vol% have larger values. Oxygen diffusivities in high-zirconia composites were thus about 8 orders of magnitude higher than those in low-zirconia composites. Furthermore, oxygen diffusivities in the low-zirconia composites (~10^{-21} to 10^{-18} m^2/s at 1000 to 1350 °C) were close to that in pure mullite, while those in the high-zirconia composites (~10^{-11} to 10^{-10} m^2/s at 1000 to 1350 °C) were close to that of zirconia.[13] It was also noted that oxygen diffusivity in mullite was unexpectedly larger than that in MZY05 or MZY15. This fact was attributed to the glassy phase typically at mullite grain triple junctions and grain boundaries because of the excess silica in mullite. It was believed that the oxygen transport through these grain boundaries, where the glassy phase was amorphous or liquidized at 1000 to 1350 °C, was easier than through a crystalline phase.

Figure 2 illustrates the relationship of oxygen diffusivities with respect to zirconia content at different temperatures, indicating that there was a dramatic increase in oxygen diffusivities between 30 and 40 vol% zirconia at all the annealing temperatures. The dramatic change in oxygen diffusivities between MZY30 and MZY40 could be explained by the percolation theory[16,17] and the effective medium theory.[18]

Bruggeman's symmetric effective medium theory assumes that two spherical particles are randomly mixed in the media. The diffusivity of such a random mixture (m), consisting of a high-diffusivity phase (h) and a low-diffusivity phase (l), can be predicted as D_m = order of D_l, if $f < f_c$ and D_m = order of D_h, if $f > f_c$, where f is the volume fraction of the high-diffusivity phase and f_c is the percolation threshold. The percolation threshold f_c occurs at the volume fraction 0.33 for a three-dimensional case.

For the conductivity of a polymer–metal composite, the threshold decreased with increasing particle size ratio of the polymer with respect to the metal, as indicated in a previous study.[19] Carmona et al.[20] observed that the threshold decreased with increasing aspect ratio of carbon fibers in the carbon–polymer composites.

In the present study, the high-diffusivity zirconia and the low-diffusivity mullite were equiaxed (or spherical) and both powders were randomly mixed. Therefore, the critical volume fraction between 30 and 40 vol% zirconia observed in this study is in agreement with the threshold

TABLE II. Measured oxygen diffusivities (D), surface exchange coefficients (α), and characteristic time constants (τ) in various composites.

Sample	Temperature (°C)	Time (s)	D (m^2/s)	α (m/s)	τ (s)[a]	t/τ
M	1000	18000	3.3×10^{-21}	2.2×10^{-13}	6.60×10^{4}	2.73×10^{-1}
MZY05	1000	18000	1.7×10^{-21}	1.3×10^{-13}	1.03×10^{5}	1.76×10^{-1}
MZY15	1000	18000	3.6×10^{-21}	1.3×10^{-13}	2.04×10^{5}	8.81×10^{-2}
MZY20	1000	18000	1.6×10^{-20}	3.6×10^{-13}	1.25×10^{5}	1.44×10^{-1}
MYZ30	1000	18000	2.2×10^{-20}	2.4×10^{-13}	3.93×10^{5}	4.57×10^{-2}
MZY40	1000	18000	1.4×10^{-12}	1.3×10^{-9}	9.13×10^{5}	1.97×10^{-2}
MYZ80	1000	18000	3.8×10^{-12}	2.9×10^{-9}	4.46×10^{5}	4.04×10^{-2}
M	1200	10800	4.8×10^{-20}	2.5×10^{-13}	7.85×10^{5}	1.38×10^{-2}
MZY05	1200	10800	2.2×10^{-20}	1.1×10^{-13}	1.93×10^{6}	5.60×10^{-3}
MZY15	1200	10800	3.3×10^{-20}	1.6×10^{-13}	1.31×10^{6}	8.24×10^{-3}
MZY20	1200	10800	1.1×10^{-19}	2.6×10^{-13}	1.56×10^{6}	6.92×10^{-3}
MZY30	1200	10800	1.3×10^{-19}	2.0×10^{-13}	3.10×10^{6}	3.48×10^{-3}
MYZ40	1200	10800	2.1×10^{-11}	1.2×10^{-9}	1.34×10^{7}	8.06×10^{-4}
MYZ80	1200	10800	3.4×10^{-11}	2.0×10^{-9}	8.23×10^{6}	1.31×10^{-3}
M	1350	7200	1.1×10^{-18}	7.1×10^{-13}	2.21×10^{6}	3.25×10^{-3}
MZY05	1350	7200	5.6×10^{-19}	4.8×10^{-13}	2.44×10^{6}	2.95×10^{-3}
MZY15	1350	7200	6.4×10^{-19}	5.8×10^{-13}	1.90×10^{6}	3.79×10^{-3}
MZY20	1350	7200	1.4×10^{-18}	6.8×10^{-13}	3.09×10^{6}	2.33×10^{-3}
MZY30	1350	7200	2.6×10^{-18}	8.4×10^{-13}	3.68×10^{6}	1.96×10^{-3}
MZY40	1350	7200	6.4×10^{-11}	2.6×10^{-9}	9.75×10^{6}	7.38×10^{-4}
MZY80	1350	7200	1.9×10^{-10}	3.2×10^{-9}	1.78×10^{7}	4.04×10^{-4}

[a]$\tau = D/\alpha^2$.

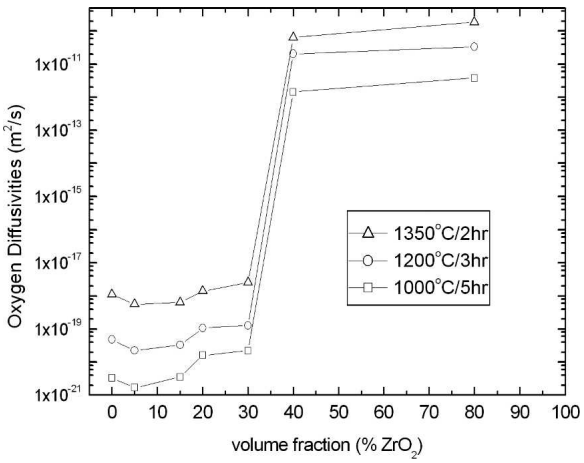

FIG. 2. The relationships of oxygen diffusivity and zirconia content after annealing at 1350 °C/2 h, 1200 °C/3 h, and 1000 °C/5 h, respectively.

value predicted by Bruggeman's symmetric effective medium theory.

Based on the measurements of silica layer (i.e., oxidation product of silicon carbide) thickness at various depths beneath the outermost surface, Lin et al.[10] phenomenologically proposed two distinct oxidation modes of silicon carbide/zirconia/mullite composites at elevated temperatures. Mode I shows a large gradient and a shallow oxidation depth, while mode II exhibits a rather small gradient and a large oxidation depth.

Lin et al.[10] claimed that the oxidation behavior strongly depended on the relative oxygen diffusivities through the silica layer and the mullite/zirconia matrix as well, even though oxygen diffusivities in various matrices were not measured at all. In their proposal, mode I was based on the assumption that oxygen diffusion in the silica layer was much faster than in the mullite/zirconia matrix, while mode II was based on the opposite assumption.

The measured oxygen diffusivities in low-zirconia composites ($\leqslant$30 vol% ZrO_2) were smaller by 3 to 4 orders of magnitude than that in SiO_2 (about 10^{-18} m^2/s at 1000 °C),[21] while those in high-zirconia composites ($\geqslant$40 vol% ZrO_2) were higher by 5 to 6 orders of magnitude than that in SiO_2. These results could validate the modeling of oxidation modes proposed by Lin et al.[10]

It was worth noting that the ^{18}O concentration profiles in the present study resemble the SiO_2 layer thickness versus depth curves reported by Tsai and Lin.[9] Both experimental results (i.e., concentration profiles and SiO_2 layer thickness) of high-zirconia composites illustrated small gradients and large diffusion (or oxidation) depths, and vice versa. It was thus concluded that the oxidation behavior of silicon carbide/zirconia/mullite composites is closely related to the oxygen diffusion through their respective zirconia/mullite matrices.

Fielitz and Borchardt[22] have discussed the working limits of the diffusivities and surface exchange coefficients determined with the SIMS depth profile. They indicated that the chosen annealing time (t) with respect to the characteristic time constant (τ) was restricted to the range: $3 \times 10^{-4} \leqslant t/\tau \leqslant 10$ if the ^{18}O concentration at the surface reached about 80% of the gas atmosphere and the

dynamic range of the ^{18}O concentration was at least 1 order of magnitude higher than the natural abundance. The ratios of the experimental annealing time (t) to the characteristic time constant (τ) are listed in Table II. It indicates that the t/τ ratios between 4.04×10^{-4} and 2.73×10^{-1} are in the limited range with sufficiently long annealing time so that the diffusivities and the surface exchange coefficients determined by Eq. (2) have acceptable accuracies in the present study.

C. Activation energies versus zirconia contents

Figure 3 displays the Arrhenius plots of oxygen diffusivities versus $1/T$ for the composites with various zirconia contents. The activation energies of oxygen diffusion in the composites were determined by the slope of fitting lines and are listed in Table III. The activation energy of oxygen diffusion in MZY40 was close to that in MZY80, while the activation energy of oxygen diffusion in MZY05 approached that in pure mullite. It was noted that the activation energy had a tendency to decrease with increasing zirconia content. However, the activation energy of oxygen diffusion in MZY30 was slightly larger than that in MZY20. The pre-exponential constant D_0 in the oxygen diffusivity expression $D = D_0 \exp(-Q/RT)$ was determined from the intercept of the ln D versus $1/T$ plot, and the results are listed in Table III. It indicates much higher D_0 values for MZY40 and MZY80 than for others.

D. Microstructural characteristics

The variation of oxygen diffusivities with respect to the zirconia content can be explained from the microstructural viewpoint. Figures 4(a) and 4(b) show the SEM micrographs of a low-zirconia and a high-zirconia composite, i.e., MZY15 and MZY40, respectively. The bright phase is zirconia, while the dark one is mullite. Figure 4(a) reveals that the zirconia particles of MZY15 were isolated in the mullite matrix. In the low-zirconia composites, the oxygen diffused mainly via the continuous mullite, which has a small oxygen diffusivity (about 10^{-21} m^2/s at 1000 °C). This is why the oxygen diffusivities in low-zirconia composites were expected to be of the same order of the oxygen diffusivity in mullite. In contrast, Fig. 4(b) shows that the zirconia particles in MZY40 were interconnected. This interconnected

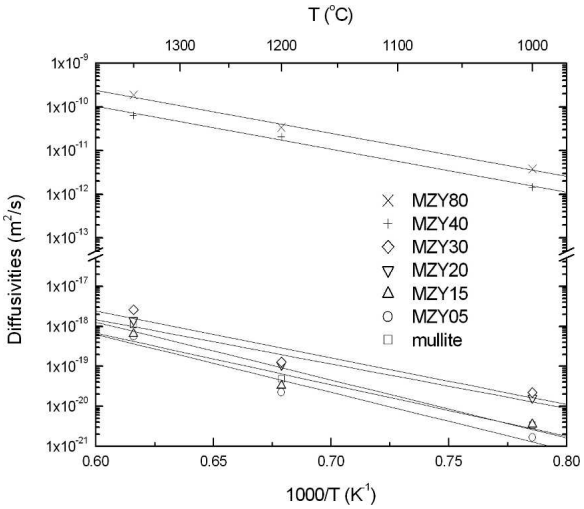

FIG. 3. Arrhenius plots of oxygen diffusivities in the composites with various zirconia contents.

TABLE III. Pre-exponential constants (D_0) and activation energies (Q) in various composites.

	D_0 (m^2/s)[a]	Q (kJ/mol)
M	$6.7\ (\pm 0.50) \times 10^{-10}$	277 (±24)
MZY05	$2.9\ (\pm 0.26) \times 10^{-10}$	277 (±29)
MZY15	$3.5\ (\pm 0.38) \times 10^{-11}$	246 (±33)
MZY20	$6.4\ (\pm 0.79) \times 10^{-12}$	212 (±30)
MZY30	$2.4\ (\pm 0.36) \times 10^{-11}$	223 (±48)
MZY40	$8.1\ (\pm 0.38) \times 10^{-5}$	188 (±15)
MZY80	$2.0\ (\pm 0.10) \times 10^{-4}$	189 (±14)

[a]$D = D_0 \exp(-Q/RT)$.

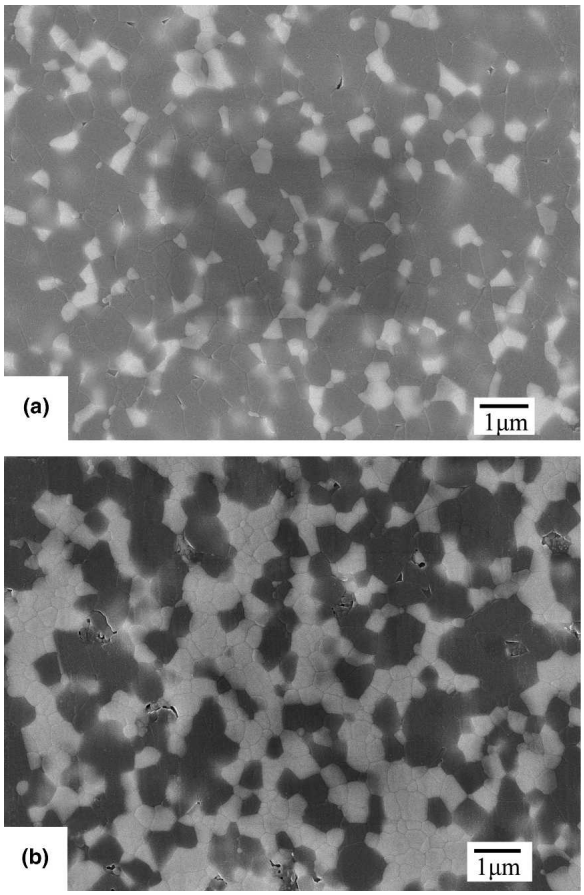

FIG. 4. Secondary electron images of the as hot-pressed (a) MZY15 and (b) MZY40. The bright phase is zirconia, while the dark phase is mullite. Thermal etching at 1300 °C/1 h.

channel of the zirconia phase, which had a high oxygen diffusivity of about 10^{-11} m^2/s at 1000 °C,[13] became a rapid diffusion path for oxygen in high-zirconia composites. It is thus expected that the oxygen diffusivities in high-zirconia composites are of the same order as the oxygen diffusivity in zirconia.

IV. CONCLUSIONS

(1) The oxygen diffusivities in various mullite/zirconia composites were measured by the $^{18}O/^{16}O$ isotope exchange and secondary ion mass spectrometry method. The oxygen diffusivities in mullite/zirconia composites ranged from 10^{-21} to 10^{-10} m^2/s, depending on the zirconia content and temperature.

(2) The oxygen diffusivities in mullite/zirconia composites exhibited a threshold of zirconia content at between 30 and 40 vol%. The high-zirconia composites showed relatively high oxygen diffusivities, close to the oxygen diffusivity in zirconia. Correspondingly, the low-zirconia composites showed relatively small oxygen diffusivities, close to the oxygen diffusivity in mullite.

(3) There was a clear tendency of the activation energies of oxygen diffusion in composites to decrease with increasing zirconia contents. The activation energies of oxygen diffusion in high-zirconia composites were close to that of zirconia; while those of low-zirconia composites approached that of mullite.

(4) The extreme difference in oxygen diffusivities between low-zirconia and high-zirconia composites was explained by the microstructural features of the composites. In the high-zirconia composites, the relatively large oxygen diffusivities were attributed to the interconnected zirconia channels, which provided a fast diffusion path for oxygen.

ACKNOWLEDGMENTS

The authors are grateful to Dr. Xue-Feng Lin and Dr. Vivian Ding at Evans Analytical Group for the SIMS measurements. The research was supported by National Science Council of Taiwan under Contract No. NSC 91-2216-E-009-021.

REFERENCES

1. M.I. Osendi, B.A. Bender, and D. Lewis, III: Microstructure and mechanical properties of mullite–silicon carbide composites. *J. Am. Ceram. Soc.* **72,** 1049 (1989).
2. R. Ruh, K.S. Mazdiyasni, and M.G. Mendiratta: Mechanical and microstructural characterization of mullite and mullite–SiC–whisker and ZrO_2-toughened-mullite–SiC-whisker composites. *J. Am. Ceram. Soc.* **71,** 503 (1988).
3. N. Claussen and J. Jahn: Mechanical properties of sintered, in situ-reacted mullite–zirconia composites. *J. Am. Ceram. Soc.* **63,** 228 (1980).
4. P.F. Becher, C.H. Hsueh, P. Angelini, and T.N. Tiegs: Toughening behavior in whisker-reinforced ceramic matrix composites. *J. Am. Ceram. Soc.* **71,** 1050 (1988).
5. C.Y. Tsai, C.C. Lin, A. Zangvil, and A.K. Li: Effect of zirconia content on the oxidation behavior of silicon carbide/zirconia/mullite composites. *J. Am. Ceram. Soc.* **81,** 2413 (1998).
6. C.C. Lin, A. Zangvil, and R. Ruh: Microscopic mechanisms of oxidation in SiC–whisker-reinforced mullite/ZrO_2 matrix composites. *J. Am. Ceram. Soc.* **82,** 2833 (1999).
7. C.C. Lin, A. Zangvil, and R. Ruh: Phase evolution in silicon carbide-whisker-reinforced mullite/zirconia composite during long-term oxidation at 1000 °C to 1350 °C. *J. Am. Ceram. Soc.* **83,** 1797 (2000).
8. P. Mogilevsky and A. Zangvil: Modeling of oxidation behavior of SiC-reinforced ceramic matrix composites. *Mater. Sci. Eng., A* **262,** 16 (1999).
9. C.Y. Tsai and C.C. Lin: Dependence of oxidation modes on zirconia content in silicon carbide/zirconia/mullite composites. *J. Am. Ceram. Soc.* **81,** 3150 (1998).
10. C.C. Lin, A. Zangvil, and R. Ruh: Modes of oxidation in SiC-reinforced mullite/ZrO_2 composites: Oxidation vs depth behavior. *Acta Mater.* **47,** 1977 (1999).
11. P. Fielitz, G. Borchardt, M. Schmucker, H. Schneider, M. Wiedenbeck, D. Rhede, S. Weber, and S. Scherrer: Secondary ion mass spectroscopy study of oxygen-18 tracer diffusion in 2/1-mullite single crystals. *J. Am. Ceram. Soc.* **84,** 2845 (2001).
12. Y. Ikuma, E. Shimada, S. Sakano, M. Oishi, M. Yokoyama, and Z. Nakagawa: Oxygen self-diffusion in cylindrical single-crystal mullite. *J. Electrochem. Soc.* **146,** 4672 (1999).
13. B.K. Kim, S.J. Park, and H. Hamaguchi: Raman spectrometric determination of the oxygen self-diffusion coefficients in oxide. *J. Am. Ceram. Soc.* **77,** 2648 (1994).
14. J. Crank: *The Mathematics of Diffusion,* 2nd ed. (Oxford University Press, New York, 1975).
15. P. Fielitz, G. Borchardt, M. Schmucker, and H. Schneider: How to measure volume diffusivities and grain boundary diffusivities of oxygen in polycrystalline oxides. *Solid State Ionics* **160,** 75 (2003).
16. S. Kirkpatrick: Percolation and conduction. *Rev. Mod. Phys.* **45,** 574 (1973).
17. V.K.S. Shante and S. Kirkpatrick: An introduction to percolation theory. *Adv. Phys.* **20,** 325 (1971).
18. R. Landauer: Electrical conductivity in inhomogeneous media, in *American Institute of Physics Conference Proceedings, No. 40, Electrical Transport and Optical Properties of Inhomogeneous Media,* edited by J.C. Garland and D.B. Tanner (American Institute of Physics, New York, 1978), p. 2.
19. R.P. Kusy: Influence of particle size ratio on the continuity of aggregates. *J. Appl. Phys.* **48,** 5301 (1977).
20. F. Carmona, R. Canet, and P. Delhaes: Piezoresistivity of heterogeneous solids. *J. Appl. Phys.* **61,** 2550 (1987).
21. E.L. Williams: Diffusion of oxygen in fused silica. *J. Am. Ceram. Soc.* **48,** 190 (1965).
22. P. Fielitz and G. Borchardt: On the accurate measurement of oxygen self-diffusivities and surface exchange coefficients in oxides via SIMS depth profiling. *Solid State Ionics* **144,** 71 (2001).